This is a post-peer-review, pre-copyedit version of an article published in **2019 13th European Conference on Antennas and Propagation (EuCAP)**. The final authenticated version is available online at: https://ieeexplore.ieee.org/document/8740245

Quasi-analytical Near-to-Far Field Transformation Based on Field Matching Method for Scattering Problems

Malgorzata Warecka[1], Piotr Kowalczyk[1], Rafal Lech[1],

[1]Faculty of Electronics, Telecommunications and Informatics, Gdansk University of Technology, Gdansk, Poland
email: warecka.malgorzata@gmail.com

***Abstract*—A new quasi-analytical near-to-far field transformation based on field matching method (field expansion in a base of Hankel functions) is presented. This approach uses finite element method to obtain near field, then the field is expressed in a base of Hankel functions. The evaluated coefficients allow to calculate the field outside the numerical domain, also in a far distance. The main advantage of the proposed technique is avoiding of the Green's function integration. The method can be applied for obstacles of an arbitrary cross section and homogeneous in one direction. In order to confirm the validity of the presented technique three different structures were analyzed and the results were verified with the other methods.**

***Index Terms*—Cylindrical structure, Near-to-far field transformation, Scattering.**

I. Introduction

Scattering problems arise in both microwaves and optic fields and have been investigated for many decades. Since then many different approaches, depending on the analyzed structures, have been developed. For structures, for which a description in the orthogonal coordinate system using constants coordinates is possible (e.g. cylindrical or elliptical rods), analytical methods can be utilized [1], [2]. These techniques are undoubtedly highly efficient (the numerical cost is low). However, they are rather inflexible from a practical point of view due to simple geometries. For more complex structures there is a number of integral equation methods [3]–[5]. These techniques require electric and magnetic currents introduction and the use of Green's function. Integration of this function may cause problems related to singularities in its domain [6]. Moreover, the efficiency of these methods are very sensitive to choice of a base, which describes the currents. In some cases the Green's functions can be omitted and field matching method can be applied [7]. However, it is restricted only to a convex cross section of the obstacle. The third class of techniques are discrete methods (e.g. finite element method [8], finite difference method [9]), which are the most versatile. In this group of techniques a numerical domain has to be limited. The truncation of the domain can cause some problems and affect the accuracy of the results. Also in these methods Green's function is utilized to far field evaluation, which can lead to aforementioned inconvenience.

In this paper, near-to-far field transformation based on field matching method (expansion in a base of Hankel functions) is presented. In the first step finite element method (FEM) is utilized to calculate the near field, then the obtained scattered field is used to calculate coefficients, which are the weights of Hankel functions of corresponding orders. The obtained coefficients allow to evaluate the field directly in any arbitrary distance (especially in far zone), in opposite to Green's function techniques where a calculation of the field in a single point (e.g. in far field) requires separate integration.

The method was verified for three exemplary structures and the results were compared with the ones obtained from different established techniques (analytical, field matching and finite difference).

II. Formulation of the Problem

A. Assumptions

The problem concerns scattering on a homogeneous cylindrical object with an arbitrary cross section. The wave can illuminate the structure at any angle (problem 2.5D)

$$\vec{E}^i = \vec{E}_0 e^{-\mathrm{j}\vec{k}\circ\vec{r}}, \tag{1}$$

where

$$\begin{aligned}\vec{E}_0 = E_0[&\cos\theta_0\cos\varphi_0\cos\psi_0 - \sin\varphi_0\sin\psi_0,\\ &\cos\theta_0\sin\varphi_0\cos\psi_0 + \cos\varphi_0\sin\psi_0, -\sin\theta_0\cos\psi_0],\end{aligned} \tag{2}$$

$$\vec{k} = k_0[\sin\theta_0\cos\varphi_0, \sin\theta_0\sin\varphi_0, \cos\theta_0] \tag{3}$$

and $k_0 = \omega/c$, where ω is angular frequency and c is light velocity in vacuum. We assume that the structure is homogeneous along z axis and variation along this direction is known; for electric field

$$\vec{E}(x,y,z) = \vec{E}(x,y)e^{-\gamma z} \tag{4}$$

and magnetic field

$$\vec{H}(x,y,z) = \vec{H}(x,y)e^{-\gamma z}, \tag{5}$$

where $\gamma = k_0\cos\theta_0$. Separating the fields to longitudinal and transversal components in Maxwell equations we obtain two coupled relations. The first one for scalar component E_z

$$\begin{aligned}\vec{\nabla}_t\circ(\vec{i}_z\times\bar{\mu}_r^{-1}\vec{i}_z\times\vec{\nabla}_t E_z) + \gamma\vec{\nabla}_t\circ(\vec{i}_z\times\bar{\mu}_r^{-1}\vec{i}_z\times\vec{E}_t)\\ = \omega^2\mu_0\varepsilon_0\varepsilon_{rz}E_z\end{aligned} \tag{6}$$

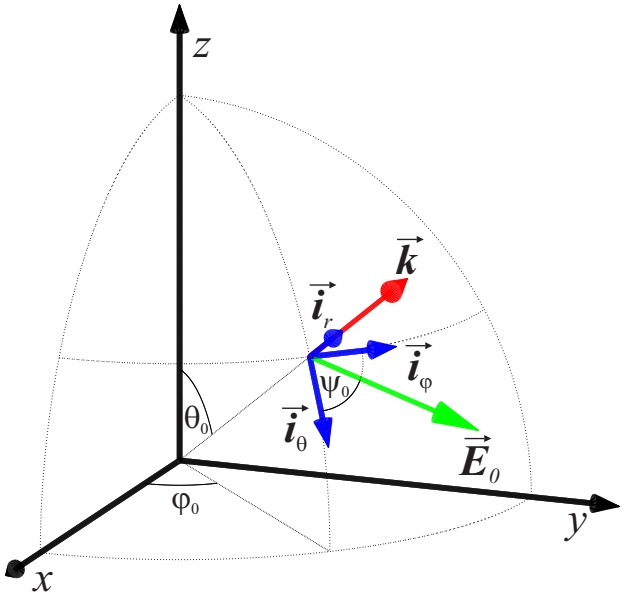

Fig. 1. Incident wave.

and the second one for vector $\vec{E}_t$

$$\begin{aligned}&\vec{\nabla}_t \times \mu_{rz}^{-1}\vec{\nabla}_t \times \vec{E}_t + \gamma\vec{i}_z \times \bar{\mu}_r^{-1}\vec{i}_z \times \vec{\nabla}_t E_z \\ &+ \gamma^2\vec{i}_z \times \bar{\mu}_r^{-1}\vec{i}_z \times \vec{E}_t = \omega^2\mu_0\varepsilon_0\bar{\varepsilon}_r\vec{E}_t,\end{aligned} \tag{7}$$

where $\bar{\mu}_r = \begin{bmatrix}\bar{\mu}_{rt} & 0\\ 0 & \mu_{rz}\end{bmatrix}$ is relative permeability, $\bar{\varepsilon}_r = \begin{bmatrix}\bar{\varepsilon}_{rt} & 0\\ 0 & \varepsilon_{rz}\end{bmatrix}$ relative permittivity, μ_0 and ε_0 are permeability and permittivity of the vacuum, respectively, and $\vec{\nabla}_t = \frac{\partial}{\partial_x}\vec{i}_x + \frac{\partial}{\partial_y}\vec{i}_y$.

B. Near-field evaluation with the use of FEM

The equations (6) and (7) can be transformed to the weak form as follows [10]

$$\begin{aligned}&-\iint_S (\vec{\nabla}_t F(x,y)) \circ (\vec{i}_z \times \bar{\mu}_r^{-1}\vec{i}_z \times \vec{\nabla}_t E_z)\, ds \\ &-\gamma\iint_S (\vec{\nabla}_t F(x,y)) \circ (\vec{i}_z \times \bar{\mu}_r^{-1}\vec{i}_z \times \vec{E}_t)\, ds \\ &-\omega^2\mu_0\varepsilon_0\iint_S F(x,y)\varepsilon_{rz}E_z\, ds = 0\end{aligned} \tag{8}$$

and

$$\begin{aligned}&\iint_S (\vec{\nabla}_t \times \vec{\mathcal{F}}(x,y)) \circ (\mu_{rz}^{-1}\vec{\nabla}_t \times \vec{E}_t)\, ds \\ &+\gamma\iint_S \vec{\mathcal{F}}(x,y) \circ (\vec{i}_z \times \bar{\mu}_r^{-1}\vec{i}_z \times \vec{\nabla}_t E_z)\, ds \\ &+\gamma^2\iint_S \vec{\mathcal{F}}(x,y) \circ (\vec{i}_z \times \bar{\mu}_r^{-1}\vec{i}_z \times \vec{E}_t)\, ds \\ &= \omega^2\mu_0\epsilon_0\iint_S \vec{\mathcal{F}}(x,y) \circ \bar{\varepsilon}_r\vec{E}_t\, ds,\end{aligned} \tag{9}$$

where $F(x,y)$ and $\vec{\mathcal{F}}(x,y)$ are the weight functions and S represents the numerical domain. For scattering problems the field can be written as a sum of incident field $\vec{E}^i$ (known) and scattered field $\vec{E}^s$ (unknown).

Applying the second order scalar $\alpha_{(n)}^{[q]}$ and vector (Whitney) $\vec{W}_{(n)}^{[q]}$ shape functions [8], [10] the fields can be expressed

$$E_z^s = \sum_{q=1}^{Q}\sum_{i=1}^{6}\psi_{(i)}^{[q]}\alpha_{(i)}^{[q]}, \quad \vec{E}_t^s = \sum_{q=1}^{Q}\sum_{i=1}^{8}\phi_{(i)}^{[q]}\vec{W}_{(i)}^{[q]}, \tag{10}$$

where Q is a number of elements. Then utilizing Galerkin method we obtain matrix equation

$$\begin{bmatrix}\mathbf{G}_{zz} & \mathbf{G}_{zt}\\ \mathbf{G}_{tz} & \mathbf{G}_{tt}\end{bmatrix}\begin{bmatrix}\Psi\\ \Phi\end{bmatrix} = \begin{bmatrix}\mathbf{P}_z\\ \mathbf{P}_t\end{bmatrix}, \tag{11}$$

where specific blocks of the matrices are defined below:

$$\begin{aligned}\left[\mathbf{G}_{zz}^{[q]}\right]_{ji} &= -\iint_{S^{[q]}} (\vec{\nabla}_t\alpha_{(j)}^{[q]}) \circ (\vec{i}_z \times \bar{\mu}_r^{-1}\vec{i}_z \times \vec{\nabla}_t\alpha_{(i)}^{[q]})\, ds,\\ \left[\mathbf{G}_{zt}^{[q]}\right]_{ji} &= -\gamma\iint_{S^{[q]}} (\vec{\nabla}_t\alpha_{(j)}^{[q]}) \circ (\vec{i}_z \times \bar{\mu}_r^{-1}\vec{i}_z \times \vec{W}_{(i)}^{[q]})\, ds,\\ \left[\mathbf{G}_{tz}^{[q]}\right]_{ji} &= \gamma\iint_{S^{[q]}} \vec{W}_{(j)}^{[q]} \circ (\vec{i}_z \times \bar{\mu}_r^{-1}\vec{i}_z \times \nabla_t\alpha_{(i)}^{[q]})\, ds,\\ \left[\mathbf{G}_{tt}^{[q]}\right]_{ji} &= \iint_{S^{[q]}} (\vec{\nabla}_t \times \vec{W}_{(j)}^{[q]}) \circ (\mu_{rz}^{-1}\vec{\nabla}_t \times \vec{W}_{(i)}^{[q]})\, ds\\ &\quad -\omega^2\mu_0\epsilon_0\iint_{S^{[q]}} \vec{W}_{(j)}^{[q]} \circ \bar{\epsilon}_r\vec{W}_{(i)}^{[q]}\, ds\\ &\quad +\gamma^2\iint_{S^{[q]}} \vec{W}_{(j)}^{[q]} \circ (\vec{i}_z \times \bar{\mu}_r^{-1}\vec{i}_z \times \vec{W}_{(i)}^{[q]})\, ds,\\ [\mathbf{P}_z^{[q]}]_{ji} &= \iint_{S^{[q]}} (\vec{\nabla}_t\alpha_{(j)}^{[q]}) \circ (\vec{i}_z \times \tilde{\bar{\mu}}_r^{-1}\vec{i}_z \times \vec{\nabla}E_z^i)\, ds\\ &\quad +\omega^2\mu_0\varepsilon_0\iint_{S^{[q]}} \alpha_{(j)}^{[q]}\tilde{\varepsilon}_{rz}E_z^i\, ds\\ &\quad +\gamma\iint_{S^{[q]}} (\vec{\nabla}_t\alpha_{(j)}^{[q]}) \circ (\vec{i}_z \times \tilde{\bar{\mu}}_r^{-1}\vec{i}_z \times \vec{\nabla}\vec{E}_t^i)\, ds,\\ \left[\mathbf{P}_t^{[q]}\right]_{ji} &= -\iint_{S^{[q]}} (\vec{\nabla}_t \times \vec{W}_{(j)}^{[q]}) \circ (\tilde{\mu}_{rz}^{-1}\vec{\nabla}_t \times \vec{E}_t^i)\, ds\\ &\quad -\gamma\iint_{S^{[q]}} \vec{W}_{(j)}^{[q]} \circ (\vec{i}_z \times \tilde{\bar{\mu}}_r^{-1}\vec{i}_z \times \vec{\nabla}_t E_z^i)\, ds\\ &\quad -\gamma^2\iint_{S^{[q]}} \vec{W}_{(j)}^{[q]} \circ (\vec{i}_z \times \tilde{\bar{\mu}}_r^{-1}\vec{i}_z \times \vec{\nabla}_t E_t^i)\, ds\\ &\quad +\omega^2\mu_0\varepsilon_0\iint_{S^{[q]}} \vec{W}_{(j)}^{[q]} \circ \tilde{\bar{\varepsilon}}_r\vec{E}_t^i\, ds\\ &\quad -\omega^2\mu_0\epsilon_0\iint_{S^{[q]}} \alpha_{(j)}^{[q]}\epsilon_{rz}\alpha_{(i)}^{[q]}\, ds.\end{aligned}$$

The vector $\begin{bmatrix}\Psi & \Phi\end{bmatrix}^T$ represents scalar and vector basis function coefficients, respectively. The numerical domain is truncated by absorbing boundary conditions - perfectly matched layer (PML). In such a case the permittivity and permeability of the structure have to be artificially modified by adding extra layers at the boundary. Since the modification do not involve the incident field permittivity ε and permeability μ in $\mathbf{P}_z$ and $\mathbf{P}_t$ matrices stay unchanged (denoted by tilda). The calculated above vector $\begin{bmatrix}\Psi & \Phi\end{bmatrix}^T$ determines the electric field in the numerical domain (near field) excluding the absorption layer.

C. Near-to-far field transformation

The obtained field can be expressed in base of Hankel functions on the circular contour surrounding the scatterer - dashed line in Fig.2. The circle has to be placed appropriately

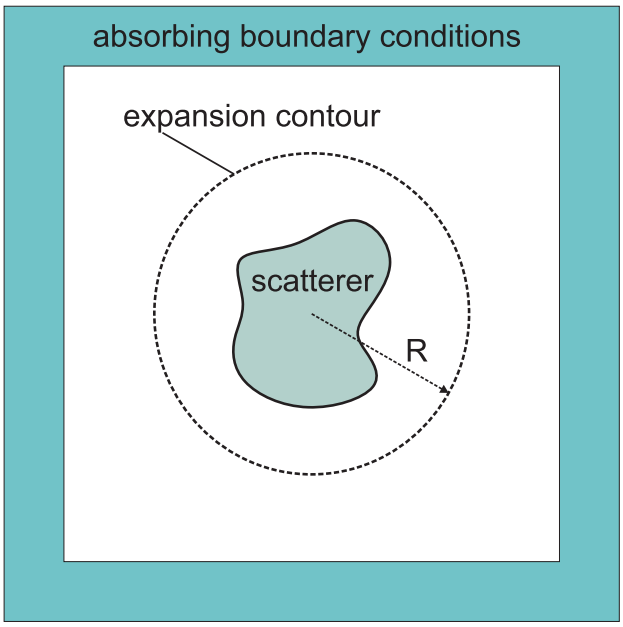

Fig. 2. Numerical domain.

outside the object and outside the absorption layer, than

$$E_z^s(\rho = R, \varphi, z = 0) = \sum_{m=-M}^{M} a_m^E H_m^{(2)}(\kappa_1 R) e^{\mathrm{j}m\varphi} \tag{12}$$

and

$$E_\varphi^s(\rho = R, \varphi, z = 0) = \sum_{m=-M}^{M} \left[\frac{-\mathrm{j}\gamma m}{\kappa_1^2 R} H_m^{(2)}(\kappa_1 R) a_m^E + \frac{\mathrm{j}\omega\mu_1}{\kappa_1} H_m'^{(2)}(\kappa_1 R) a_m^H \right] e^{\mathrm{j}m\varphi}. \tag{13}$$

The assumption of $z = 0$ do not affect the generality of the approach. The coefficients a_n^E and a_n^H can be evaluated by simple projection with the use of functions $w_n = e^{\mathrm{j}n\varphi}$ on the aforementioned circle of radius R, than

$$a_n^E = \frac{1}{2\pi H_n^{(2)}(\kappa_1 R)} \int_0^{2\pi} E_z^s(R, \varphi, 0) e^{-\mathrm{j}n\varphi}\, d\varphi \tag{14}$$

and

$$a_n^H = \frac{\kappa_1}{2\pi \mathrm{j}\omega\mu_1 H_n'^{(2)}(\kappa_1 R)} \int_0^{2\pi} E_\varphi^s(R, \varphi, 0) e^{-\mathrm{j}n\varphi}\, d\varphi + \frac{\gamma n}{\omega\mu_1\kappa_1 R H_n'^{(2)}(\kappa_1 R)} H_n^{(2)}(\kappa_1 R) a_n^E. \tag{15}$$

These coefficients are sufficient to calculate all the components of the electric and magnetic fields in any distance outside the considered circle [11]. A calculation of the field in any new point does not require any integration, in opposite to Green's function method.

III. Numerical results

To verify the presented method three examples are shown. For all considered structures the same parameter of PML is utilized. The permittivity and permeability for absorption layer is expressed by [10]

$$\bar{\boldsymbol{f}} = f_0 \boldsymbol{\Lambda}^g, \boldsymbol{\Lambda}^x = \begin{bmatrix} a & 0 & 0 \\ 0 & a^{-1} & 0 \\ 0 & 0 & a^{-1} \end{bmatrix}, \boldsymbol{\Lambda}^y = \begin{bmatrix} a^{-1} & 0 & 0 \\ 0 & a & 0 \\ 0 & 0 & a^{-1} \end{bmatrix}$$

where $f \in \{\varepsilon, \mu\}$ and $g \in \{x, y\}$; Λ^x is assigned to the border in $x = const$ and Λ^y to the border in $y = const$. For the corners of the boundaries Λ^{xy} is defined as a product of Λ^x and Λ^y. In all the presented examples the coefficient a is set to $1 - \mathrm{j}10^{10}/\omega$. All the considered objects are made of dielectric material with relative permittivity $\varepsilon_r = 5$ and placed in free space. A number of Hankel functions used in the calculations is set to $M = 10$ and maximum length of the edge in the FEM mesh is $h_{max} = 0.067\lambda$ [12]. The scattering characteristics for all cases are evaluated at the distance of 100λ.

The first considered structure is a cylinder with an elliptical cross section of geometry presented in Fig. 3. The object is

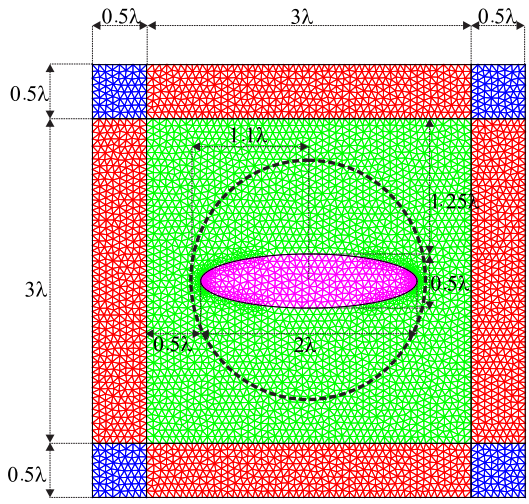

Fig. 3. Geometry of the elliptical cylinder.

surrounded with a circle of radius $R = 1.1\lambda$ (Fig. 3) and obtained characteristics are shown in Fig. 4. The solid line

represents the data calculated with the use of the proposed method and the dashed line is an analytical reference.

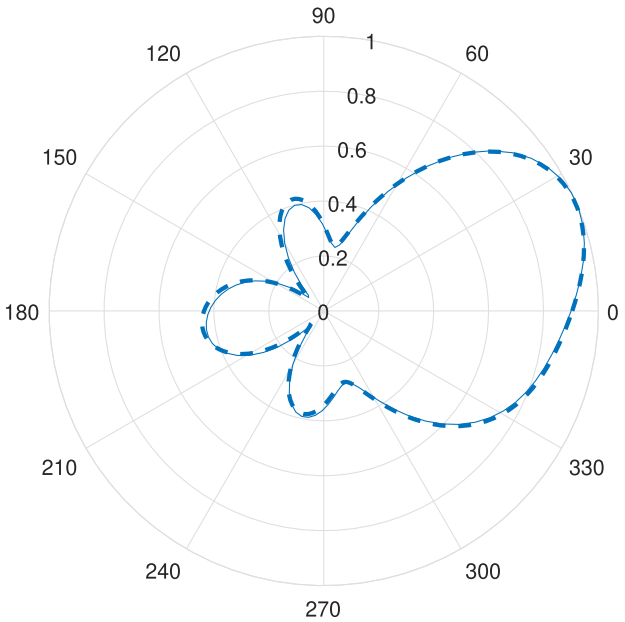

Fig. 4. Normalized scattering characteristics for elliptical cylinder (solid line - this method, dashed line - analytical results).

Next example is a cylinder with rectangular cross section, which is surrounded by contour of radius $R = 0.8\lambda$. The geometry of the structure and calculated scattering characteristics are presented in Fig.5-6 (solid line - this method, dashed line - mode matching method [7]).

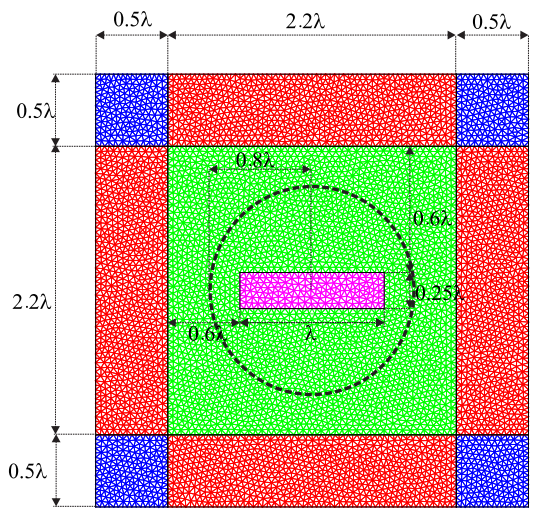

Fig. 5. Geometry of the rectangular cylinder.

As the last proposed structure, a cross-shaped cylinder is considered. The geometry parameters are presented in Fig.7. The circle of radius 0.8λ is used to expand the field in a base of Hankel functions. The obtained characteristics (solid line) and a comparison with finite difference method [13] (dashed line) are shown in Fig.8.

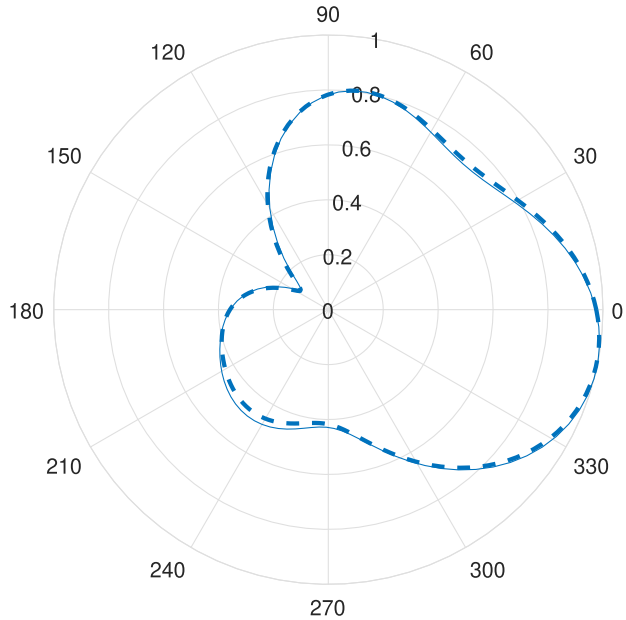

Fig. 6. Normalized scattering characteristics for rectangular cylinder (solid line - this method, dashed line - mode matching method).

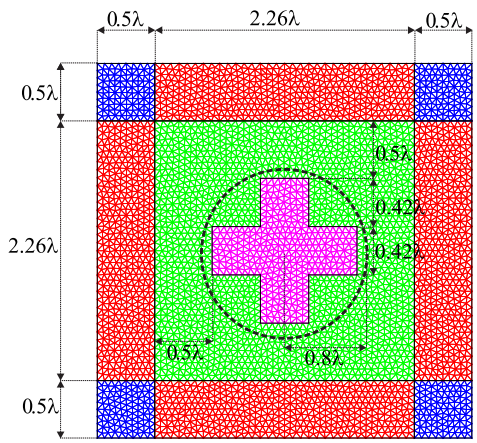

Fig. 7. Geometry of the cross-shaped cylinder.

IV. Conclusion

The field expansion in a base of Hankel functions is proposed. The presented near-to-far field transformation requires a small number of integrations which makes it fast and simple. The results are verified by comparison with alternative numerical methods and a very good agreement is achieved.

Acknowledgment

This work was supported from sources of project EDISOn - Electromagnetic Design of flexIble SensOrs carried out within the TEAM-TECH programme of the Foundation for Polish Science co-financed by the European Union under the European Regional Development Fund, Smart Growth Operational Programme 2014-2020.

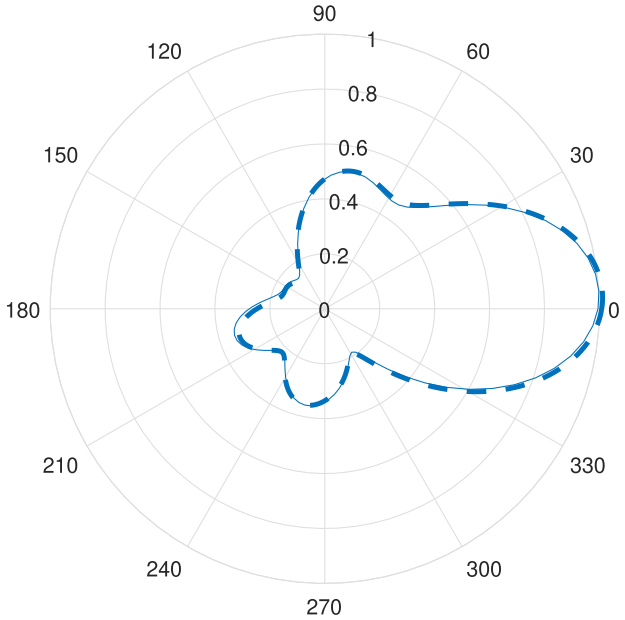

Fig. 8. Normalized scattering characteristics for cross-shaped cylinder (solid line - this method, dashed line - finite difference method).

REFERENCES

[1] Tsang L, Kong JA, Ding K-H. *Scattering of Electromagnetic Waves: Theories and Applications*, John Wiley and Sons, Inc., 2002.

[2] Bowman JJ, Senior TBA, Uslenghi PLE *Electromagnetic and Acoustic Scattering by Simples Shapes*, John Wiley and Sons, Amsterdam, 1969.

[3] A. Valero, M. Ferrando *Full-wave equivalent network representation for multiple arbitrary shaped posts in H-plane waveguide*, IEEE Transaction on Microwave Theory and Techniques, 47(10):1997-2002, 1999.

[4] G.P. Zouros, G.C. Kokkorakis, *Electromagnetic Scattering by an Inhomogeneous Gyroelectric Sphere Using Volume Integral Equation and Orthogonal Dini-Type Basis Functions*, IEEE Transactions on Antennas and Propagation, 63(6):2665-2676, 2015.

[5] Libo Wang, Lianlin Li, Yunhua Tan, *A Novel Approximate Solution for Electromagnetic Scattering by Dielectric Disks*, IEEE Transactions on Geoscience and Remote Sensing, 53(5):2948-2955, 2015.

[6] Y. Okuno, K. Yasuura *Numerical algorithm based on the mode-matching method with a singular-smoothing procedure for analyzing edge-type scattering problems*, IEEE Transactions on Antennas and Propagation, 30(4):580587, 1982.

[7] R. Lech,P. Kowalczyk,A. Kusiek *Scattering from a cylindrical object of arbitrary cross section with the use of field matching method*, IEEE Transactions on Antennas and Propagation, 64(11):4883-4887, 2016.

[8] D.B. Davidson *Computational Electromagnetics for RF and Microwave Engineering*, Cambridge University Press, 2011.

[9] A. Taflove, S.C. Hagness, *Computational Electrodynamics: The Finite-Difference Time-Domain Method*, Third Edition, Artech House, Boston and London, 2005.

[10] G. Pelosi,R. Coccioli *Quick Finite Elements for Electromagnetic Waves*, Artech House, 2009.

[11] D.M. Pozar *Microwave Engineering*, Wiley, New York, 1997.

[12] D. ngwirda *Mesh2d - delaunay-based unstructured mesh-generation*, urlhttps://www.mathworks.com/matlabcentral/fileexchange/25555-mesh2d-delaunay-basedunstructured-mesh-generation, 2009.

[13] J. Mazur,A. Kusiek,R. Lech *A new hybrid method for analysis of scattering from arbitrary configuration of cylindrical objects*, IEEE Transactions on Antennas and Propagation, 56(6):17251733, 2008.